Supplementary Information

Simulation on magneto-induced rearrangeable microstructure of magnetorheological plastomer

Taixiang Liu,[a] Xinglong Gong,*[a] Yangguang Xu,[a] Shouhu Xuan[a] and Wanquan Jiang[b]

[a] *CAS Key Laboratory of Mechanical Behavior and Design of Materials, Department of Modern Mechanics, University of Science and Technology of China, Hefei, Anhui, 230027, China*

[b] *Department of Chemistry, University of Science and Technology of China, Hefei, Anhui, 230027, China.*

*Corresponding author. E-mail: gongxl@ustc.edu.cn; Tel & Fax: 86-551-3600419.

In this supplementary information, we will discuss the origin of Eq. (8) and the reason for magneto-induced layered microstructure. Besides, considering uniaxial normal stress may be important in practical application, we present the stationary Z-axis normal stress of magnetorheological plastomer (MRP) under different changing external magnetic field.

Content:

1. The origin of Eq. (8) in 4th page of the manuscript

2. Discussion for the reason of magneto-induced layered microstructure

3. The Z-axis normal stress of MRP under fast stepwise rotating magnetic field

4. The Z-axis normal stress of MRP under stepwise rotating magnetic field from a steady state to another steady state

5. **The Z-axis normal stress of MRP under spatially changing magnetic field**

1. The origin of Eq. (8) in 4th page of the manuscript

To our knowledge, we know the magnetic point dipole approximation is not enough for computing the interactions between close large particles. Therefore, to amend the interparticle force model was our original intention. By the literature research, we found it is difficult to use the existing results directly to handle the interparticle forces in large particulate assemble. To make it, the simplest and easy-to-use way is directly to give a correction function to the dipolar approximation. Then based on the work of reference [1] bellow, we did numeric computation intending directly modify the force model on the basis of dipolar approximation. To make it clear, we honestly suggest you giving a glance at the two references:

[1] Eric E. Keaveny and Martin R. Maxey. Modeling the magnetic interactions between paramagnetic beads. *Journal of Computational Physics*, 2008, **227**, 9554. (Reference 33 in our manuscript)

Online version: http://www.sciencedirect.com/science/article/pii/S0021999108003677

[2] Barry J. Cox, Ngamta Thamwattana and James M. Hill. Electric field-induced force between two identical uncharged spheres. *Applied Physics Letters*, 2006, **88**, 152903. (This letter shows us the electric field-induced force of two spheres, which is similar to magneto-induced interparticle force of two magnetized particles)

Reference [1] compared existing methods for computing the magnetic interactions between close paramagnetic particles and described an alternative mutual finite-dipole model. The basic and general procedure to solve magnetostatic problem is introduced in section "2. Magnetostatic problem". The final expression to compute magnetostatic force is

$$\boldsymbol{F}_n = a^2 \int_0^{2\pi} \int_0^{2\pi} \mathbf{T} \cdot \hat{\boldsymbol{r}}_n \sin(\theta_n) \mathrm{d}\theta_n \mathrm{d}\phi_n \ .$$

Where a is the radius of particle. T is the Maxwell stress tensor. $\hat{r}_n$ denotes the direction of local surface. θ_n and ϕ_n denote the zenith and azimuth angles respectively for the spherical coordinate system. The mutual finite-dipole model and the numerical procedure with the mutual finite-dipole model can be get in section "3.2. Mutual finite-dipole model" (pp. 9560-9561). The compare results are shown below (Fig. 2 in reference [1])
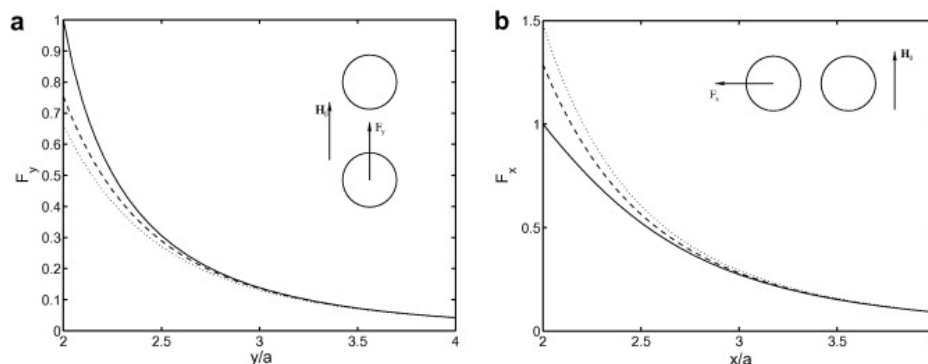

Fig. S1 Values of the interbead force for two beads in a uniform field H0=(0,1,0) with μ/μ0=5. (a) F_y as a function of separation. The values of F_y are normalized by the value of F_y of the exact solution at separation y/a=2. (b) F_x as a function of separation. The values of F_x are normalized by the value of F_x of the exact solution at separation x/a=2. The inset sketch is not drawn to scale and depicts the configuration of the beads relative to the applied field

and the direction of the measured resulting force. In the plots: (⋯) fixed dipole; (– – –) mutual dipole; (—) exact solution.

The exact force solution to the two-body problem can be found in section "4.1 Solution to the two-body problem". The sketch of two-body problem is shown in Fig. 2 as below.
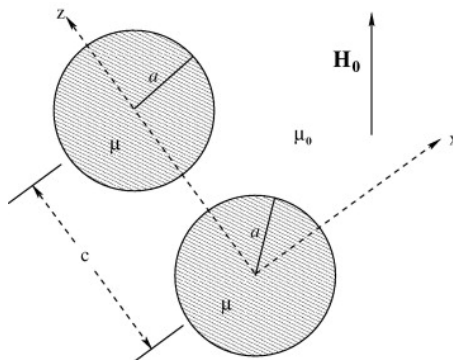

Fig. S2 The two-body problem (Fig. 8 in reference [1])

The solution of field from the other particle is (Eq. (68)-(70))

$$H_r = \sum_{l=0}^{L}\sum_{m=0}^{1}\left[(l+1)\beta_{lm}^{(1)}\frac{P_l^m(\cos\theta_1)}{r_1^{l+2}} - \beta_{lm}^{(2)}\sum_{s=m}^{L}(-1)^{s+m}\binom{l+s}{s+m}s\frac{r_1^{s-1}}{c^{l+s+1}}P_s^m(\cos\theta_1)\right]\cos m\phi,$$

$$H_\theta = -\sum_{l=0}^{L}\sum_{m=0}^{1}\left[\frac{\beta_{lm}^{(1)}}{r_1^{l+2}}\frac{dP_l^m(\cos\theta_1)}{d\theta_1} + \beta_{lm}^{(2)}\sum_{s=m}^{L}(-1)^{s+m}\binom{l+s}{s+m}\frac{r_1^{s-1}}{c^{l+s+1}}\frac{dP_s^m(\cos\theta_1)}{d\theta_1}\right]\cos m\phi,$$

$$H_\phi = \sum_{l=0}^{L}\left[\frac{\beta_{l1}^{(1)}}{r_1^{l+2}\sin\theta_1}P_l^1(\cos\theta_1) + \beta_{l1}^{(2)}\sum_{s=1}^{L}(-1)^{s+1}\binom{l+s}{s+1}\frac{r_1^{s-1}}{c^{l+s+1}\sin\theta_1}P_s^1(\cos\theta_1)\right]\sin\phi.$$

With the magnetic field known, the interparticle force can be computed after the Maxwell stress tensor is formed.

$$T_{ij} = \mu_0 H_i H_j - \frac{\mu_0}{2}\delta_{ij}H_k H_k,$$

$$F_X = \int_{r_n=a} T_{xr}\, dS,$$
$$F_y = 0,$$
$$F_z = \int_{r_n=a} T_{zr}\, dS.$$

(Eq. (10), (71)-(73) in reference [1])

Section "4.2. Inclusion of two-body effects into dipole models" in reference [1] directs us to take the two-body effect into account step by step:

1) Far-field/dipole calculation.
2) Determine if $c<R_c$.
3) Compute higher order multipoles.
4) Adjust two-body dipole moments to include far-field effects.
5) Determine the resulting field.
6) Form and evaluate the Maxwell stress tensor.
7) Correct the total magnetic force.

Hereto, we can get the two-particle interaction force with much accuracy, but it is difficult to introduce the effect directly to three-particle, four-particle… and many particles assemble. To simplify the problem, in our work, we numerically calculated the interparticle force of two particles with different interparticle angle and spacing, and then get the force error in comparison with classical point dipole model. Linear superposition is still taken to count the effect of other particles acting on a certain particle in our simulation.
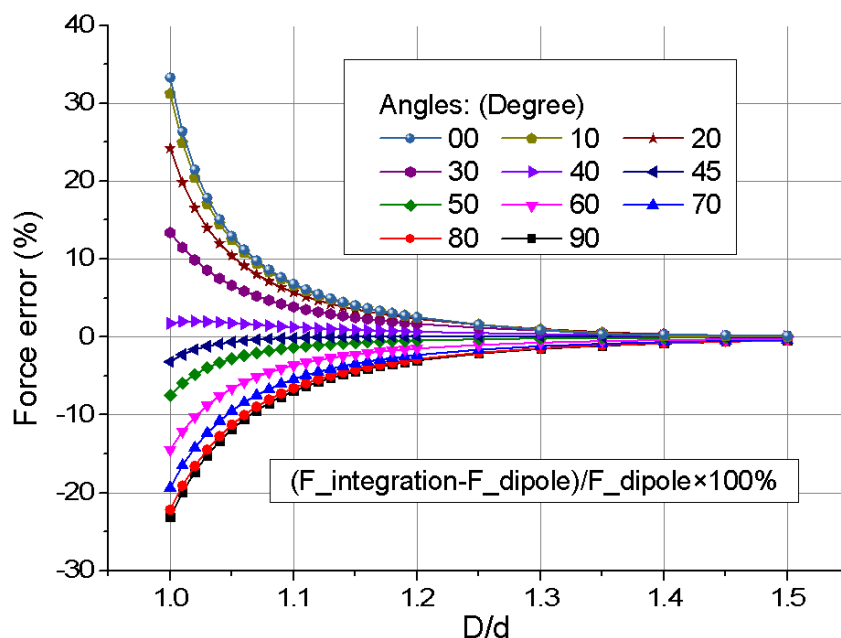

Fig. S3 Force error with different angle and interparticle spacing

(a)   (b)
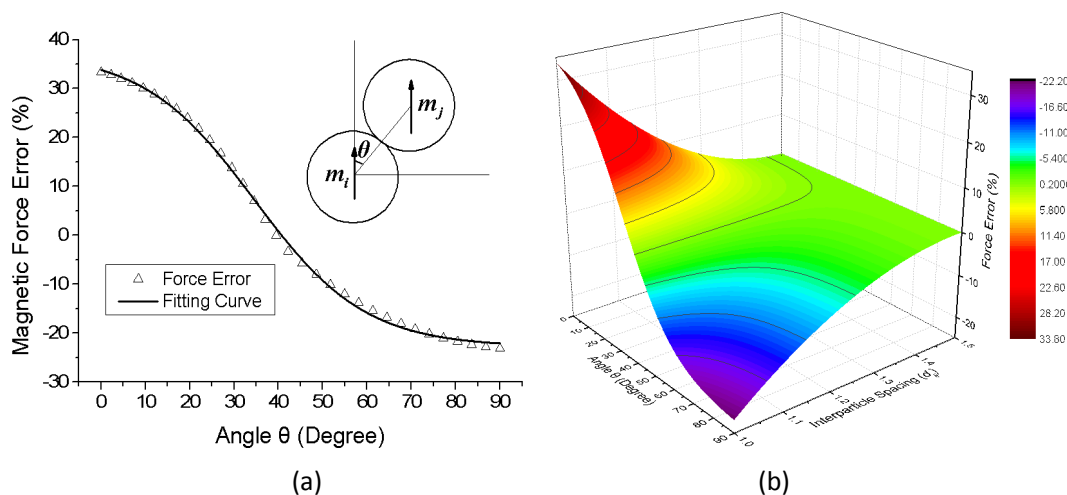
Fig. S4 Force error with different angle at D=r_{ij} (a) and different interparticle spacing (b)

Indeed, we fit the error data using OriginPro 9.0 (OriginLab Corporation, Northampton, MA 01060, USA) to give a modified force formula as:

$$F_{ij}^{m} = \begin{cases} c_m \cdot F_{ij}^{dipole}, \text{ for } d_{ij} \leq r_{ij} \leq 1.5 d_{ij} \\ F_{ij}^{dipole}, \text{ for } r_{ij} > 1.5 d_{ij} \end{cases},$$

$$c_m = 1 + \left(3 - \frac{2r_{ij}}{d_{ij}}\right)^2 \left(\frac{60.17}{1 + e^{(\theta - 34.55)/12.52}} - 22.79\right)\frac{1}{100}$$

Though we cannot give the physical meaning of the parameters at this stage, we think it is not so bad to give a simple and easy-to-use modified formula.

2. Discussion for the reason of magneto-induced layered microstructure

To simplify the analysis of the interparticle magnetic interaction, we consider giving an example in the two-dimensional situation. The illustration of the interparticle magnetic interaction model is shown as:
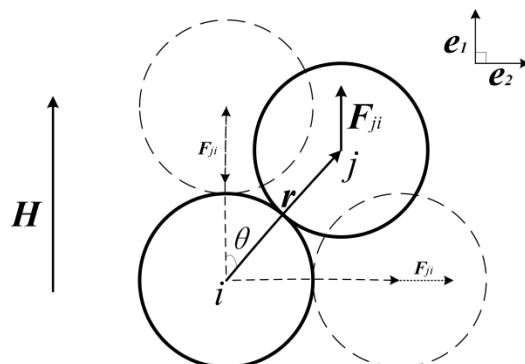

Fig. S5 The illustration of interparticle magnetic interaction

Here, we assume the magnetic moments of the two particles are both along with the external magnetic field. In Fig. S1, θ denotes the angle between the external magnetic field $\boldsymbol{H}$ and the interparticle position vector $\boldsymbol{r}$. According to the geometric symmetry, we only consider the θ being in $(0, \pi/2)$. $\boldsymbol{F}_{ji}$ is the force applied on the particle j from particle i. We define the orthogonal reference frame $\boldsymbol{e}_i$ (as shown in the top-right corner of Fig. S1) with:

$$\begin{cases} \boldsymbol{H} = H\boldsymbol{e}_1, \ \boldsymbol{r} = r_{ij}\hat{\boldsymbol{r}} = r_{ij}\left(\cos(\theta)\boldsymbol{e}_1 + \sin(\theta)\boldsymbol{e}_2\right) \\ \boldsymbol{m}_i = m_i\boldsymbol{e}_1, \ \boldsymbol{m}_j = m_j\boldsymbol{e}_1 \end{cases} \tag{1}$$

$$\boldsymbol{F}_{ji} = -\boldsymbol{F}_{ij} = \frac{c_m(r_{ij},\theta)\cdot 3\mu_0}{4\pi r_{ij}^4 \mu_1}\left[\left(\boldsymbol{m}_i\cdot\boldsymbol{m}_j\right)\hat{\boldsymbol{r}} - 5\left(\boldsymbol{m}_i\cdot\boldsymbol{r}\right)\left(\boldsymbol{m}_j\cdot\boldsymbol{r}\right)\boldsymbol{r} + \left(\boldsymbol{m}_j\cdot\boldsymbol{r}\right)\boldsymbol{m}_i + \left(\boldsymbol{m}_i\cdot\boldsymbol{r}\right)\boldsymbol{m}_j\right].$$

$$(2)$$

Then, we can have:

$$\boldsymbol{F}_{ji} = \frac{c_m(r_{ij},\theta)\cdot 3\mu_0 m_i m_j}{4\pi r_{ij}^4 \mu_1}\left[\left(3\cos(\theta) - 5\cos^3(\theta)\right)\boldsymbol{e}_1 + \left(\sin(\theta) - 5\cos^2(\theta)\sin(\theta)\right)\boldsymbol{e}_2\right]. \tag{3}$$

So we can know:

$$\begin{cases} \boldsymbol{F}_{ji} = -\dfrac{c_m(r_{ij},\theta)\cdot 3\mu_0 m_i m_j}{2\pi r_{ij}^4 \mu_1}\boldsymbol{e}_1, \ when \ \theta = 0 \\ \boldsymbol{F}_{ji} = \dfrac{c_m(r_{ij},\theta)\cdot 3\mu_0 m_i m_j}{2\pi r_{ij}^4 \mu_1}\boldsymbol{e}_2, \ when \ \theta = \dfrac{\pi}{2} \end{cases} \tag{4}$$

Eq. (4) indicates particle j is attracted by particle i when $\theta = 0$, resulting in the two particles going to be collinear along with the external magnetic field (going to be coplanar in the rotating plane of external magnetic field for three-dimensional situation). While particle j is repulsed by particle i when $\theta = \pi/2$, resulting in the two particles separating in the perpendicular direction of external magnetic field (separating along with the normal direction of the rotating plane of external magnetic field for three-dimensional situation). Therefore, there must be a critical angle θ to

be watershed to the above two phenomena. From the illustration of interparticle magnetic interaction (Fig. S1), we can easily to find the determinant condition as F_{ji} orientating to the direction of external magnetic field. To find the critical angle θ, we can have:

$$\boldsymbol{F}_{ji}^{e_2} = \frac{c_m(r_{ij},\theta)\cdot 3\mu_0 m_i m_j}{4\pi r_{ij}^4 \mu_1}\left(\sin(\theta) - 5\cos^2(\theta)\sin(\theta)\right)\boldsymbol{e}_2 = \boldsymbol{0} \quad . \tag{5}$$

Here, $\boldsymbol{F}_{ji}^{e_2}$ is the component of $\boldsymbol{F}_{ji}$ along $\boldsymbol{e}_2$ axis. That is:

$$\sin(\theta) - 5\cos^2(\theta)\sin(\theta) = 0 \quad . \tag{6}$$

Solve Eq. (6) and we can have:

$$\cos(\theta) = \sqrt{5}/5 \quad . \tag{7}$$

Therefore, for 3D situation, we can generally conclude that:

When $|\cos(\theta)| > \sqrt{5}/5$, the particles will go to be coplanar in the rotating plane of external magnetic field. When $|\cos(\theta)| < \sqrt{5}/5$, the particles will separate along the normal direction of the rotating plane of external magnetic field.

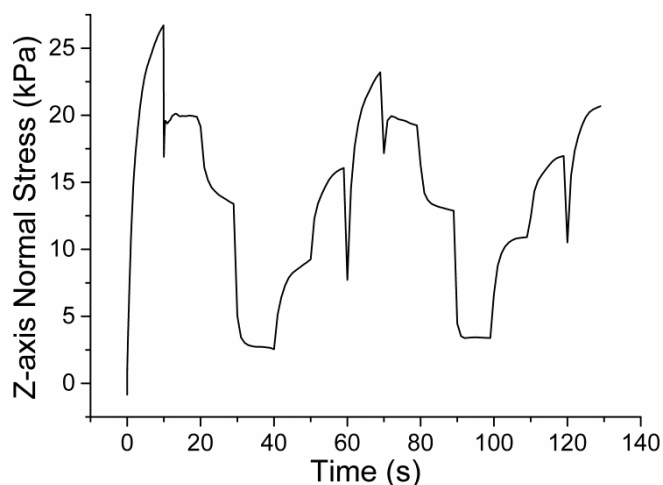### 3. The Z-axis normal stress of MRP under fast stepwise rotating magnetic field

Fig. S6 The Z-axis normal stress of MRP-70 under stepwise rotating
magnetic field with strength H=391.0 kA/m and interval △t=10 s.

Relating the evolution of microstructure shown as Fig. 12 in the main manuscript, Fig. S2 shows the Z-axis normal stress evolves over time under fast rotating magnetic field:

$$\begin{cases} \boldsymbol{H}_x = \sin(2\pi t_n /120)H \cdot \hat{\boldsymbol{x}} \\ \boldsymbol{H}_y = 0\hat{\boldsymbol{y}} \\ \boldsymbol{H}_z = \cos(2\pi t_n /120)H \cdot \hat{\boldsymbol{z}} \end{cases}$$

Here, magnetic strength H=391.0 kA/m and $t_n = t_{n-1} + \Delta t (n = 1, 2, 3 \cdots, 12)$ with initial t_0=0 s and interval Δt =10 s. With the rotating of external magnetic field, Z-axis normal stress varies periodically overall. When applying external magnetic field transiently, the axial normal stress in MRP along with the magnetic field's orientation (Z-axis) will sharply increase. This reflects the interior particle-formed microstructure of MRP has a dramatic change (from initial random isotropic dispersedness to chain-like anisotropic structure). The normal stress has an abrupt drop for a next transient rotating of external magnetic field. Meanwhile, the cusp of the normal stress appears due to the microstructure has not been stable in the previous rotating step. The Z-axis normal stress gets minimal values when the external magnetic field is perpendicular the Z-axis (at 40 s or 100 s) while gets maximal values when the external magnetic field is parallel to Z-axis (at 10 s, 70 s or 130 s).

4. The Z-axis normal stress of MRP under stepwise rotating magnetic field from a steady state to another steady state
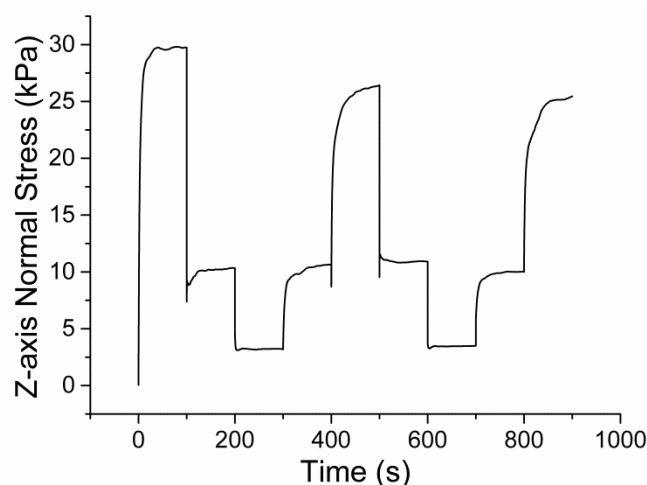

Fig. S7 The Z-axis normal stress of MRP-70 under stepwise rotating magnetic field with strength H=391.0 kA/m and interval △t=100 s.

Relating the evolution of microstructure shown as Fig. 13 in the main manuscript, Fig. S3 presents the Z-axis normal stress evolves over time under the stepwise rotating magnetic field:

$$\begin{cases} \boldsymbol{H}_x = \sin(2\pi t_n / 800)H \cdot \hat{\boldsymbol{x}} \\ \boldsymbol{H}_y = 0\,\hat{\boldsymbol{y}} \\ \boldsymbol{H}_z = \cos(2\pi t_n / 800)H \cdot \hat{\boldsymbol{z}} \end{cases}$$

Here, magnetic strength H=391.0 kA/m and $t_n = t_{n-1} + \Delta t (n = 1, 2, 3 \cdots, 8)$ with initial t_0=0 s and interval Δt=100 s. The Z-axis normal stress in MRP-70 increases sharply at the beginning of applying an external magnetic field and approaches to a certain stable value gradually. Meanwhile, the particle-formed microstructure changes from initial random dispersedness to final chain-like structure. Then rotate the external magnetic field from initial being parallel to Z-axis (in the stage of 0 s-100 s) to being perpendicular to Z-axis (in the stage of 200 s-300 s), the Z-axis normal stress decreases stage-wisely. The chain-like structure inclines to the external magnetic field gradually and is finally perpendicular to Z-axis. Continue to rotate the external magnetic field from being perpendicular to Z-axis (200-300 s stage) to being antiparallel to Z-axis (400-500 s stage), the stress increases again. With the rotating of the magnetic field, the Z-axis normal stress varies stage-wisely and periodically. The Z-axis normal stress gets maximal values in the stages of the external magnetic field being parallel to Z-axis (i. e. the stages of 0-100 s, 400-500 s, and 800-900 s) while gets minimal values when the external magnetic field is perpendicular the Z-axis (i. e. the stages of 200-300 s and 600-700 s).

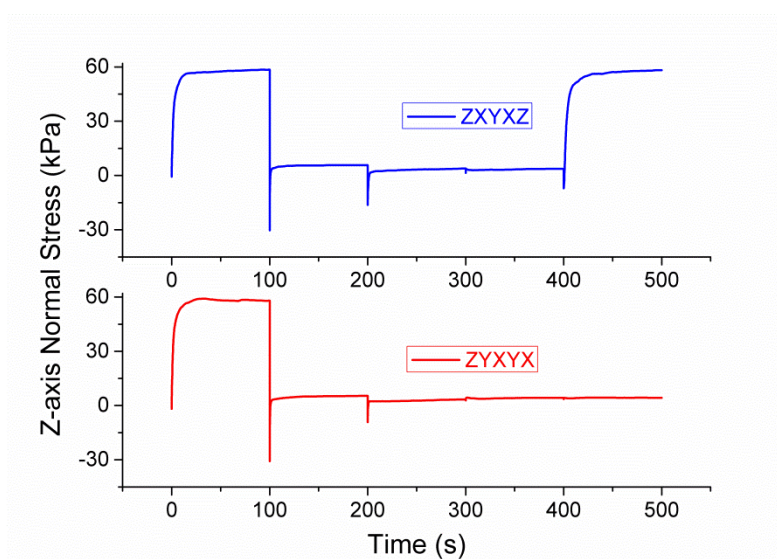## 5. The Z-axis normal stress of MRP under spatially changing magnetic field

Fig. S8 The Z-axis normal stress of MRP-70 under spatially changing magnetic field with strength H=740.1 kA/m and interval △t=100 s.

Fig. S4 shows the Z-axis normal stress of MRP-70 under spatially changing magnetic field, which relates to the evolution of microstructure shown as Fig. 17 in the main manuscript. To the upper series "ZXYXZ", the Z-axis normal stress gets sharp increase at the beginning and then quickly approaches to a stable value when suddenly applying an external magnetic field for the first 100-second stage. When transiently change the magnetic field to X axis, the Z-axis normal stress will abruptly drop down. The transient negative Z-axis normal stress at the turning point results from that the interparticle magnetic attractive force along Z-axis in the previous stage suddenly switches to interparticle magnetic repulsive force along Z-axis. Then the Z-axis normal stress keeps a small value near 0 kPa exclude the values at the turning points. The Z-axis normal stress strengthens again when the external magnetic field redirects to Z-axis. Comparing to the upper series "ZXYXZ", the nether series "ZYXYX" mainly differs in the final step. In which, the external magnetic field changes in the XY plane as same with the several previous steps. The Z-axis normal stress does not change obviously.

PS:

The GIF animations related to series "ZXYXZ" with different views is attached in "Supplementary_Information.zip" are named as "ZXYXZ-isometric_view", "ZXYXZ-top_view", and "ZXYXZ-X_view", respectively.